UCLA
UCLA Previously Published Works

Title

Guiding the osteogenic fate of mouse and human mesenchymal stem cells through feedback system control

Permalink

https://escholarship.org/uc/item/9h49t6qn

Journal

Scientific Reports, 3(1)

ISSN

2045-2322

Authors

Honda, Yoshitomo
Ding, Xianting
Mussano, Federico
et al.

Publication Date

2013

DOI

10.1038/srep03420

Peer reviewed

Guiding the osteogenic fate of mouse and human mesenchymal stem cells through feedback system control

Yoshitomo Honda[1,2,3], Xianting Ding[4,5], Federico Mussano[1,6], Akira Wiberg[1], Chih-ming Ho[4] & Ichiro Nishimura[1]

[1]The Weintraub Center for Reconstructive Biotechnology, Division of Advanced Prosthodontics, UCLA School of Dentistry, Box 951668, Los Angeles, CA, 90095, USA, [2]Craniofacial Function Engineering and Research Unit for Interface Oral Health Science, Tohoku University Graduate School of Dentistry, 4-1 Seiryo-machi, Aoba-ku, Sendai, 980-8575, Japan, [3]Institute of Dental Research, Osaka Dental University, 8-1 Kuzuha Hanazonocho, Hirakata-Shi, Osaka, 573-1121, Japan, [4]Department of Mechanical and Aerospace Engineering, UCLA Henry Samueli School of Engineering and Applied Science, 420 Westwood Plaza, Los Angeles, CA, 90095, USA, [5]Department of Biomedical Engineering, Med-X Research Institute, Shanghai Jiao Tong University, 1954 Huashan Road, Shanghai, 200030, China, [6]Department of Surgery, Dental School, University of Turin, via Nizza 230, 10127, Turin, Italy.

Correspondence and requests for materials should be addressed to I.N. (inishimura@dentistry.ucla.edu)

Stem cell-based disease modeling presents unique opportunities for mechanistic elucidation and therapeutic targeting. The stable induction of fate-specific differentiation is an essential prerequisite for stem cell-based strategy. Bone morphogenetic protein 2 (BMP-2) initiates receptor-regulated Smad phosphorylation, leading to the osteogenic differentiation of mesenchymal stromal/stem cells (MSC) *in vitro*; however, it requires supra-physiological concentrations, presenting a bottleneck problem for large-scale drug screening. Here, we report the use of a double-objective feedback system control (FSC) with a differential evolution (DE) algorithm to identify osteogenic cocktails of extrinsic factors. Cocktails containing significantly reduced doses of BMP-2 in combination with physiologically relevant doses of dexamethasone, ascorbic acid, beta-glycerophosphate, heparin, retinoic acid and vitamin D achieved accelerated *in vitro* mineralization of mouse and human MSC. These results provide insight into constructive approaches of FSC to determine the applicable functional and physiological environment for MSC in disease modeling, drug screening and tissue engineering.

With the recent advent of rapid advancements in stem cell engineering, personalized cell-based disease modeling *in vitro* plays an important role for the mechanistic elucidation of disease pathology and potential drug screening[1]. The mesenchymal stromal/stem cell (MSC) is a prototypic stem cell model exhibiting extensive proliferative ability in an uncommitted state and multi-potent differentiation capability[2]. MSCs have been used for disease modeling[3,4], tissue engineering[5,6] or high-throughput drug screening[7,8], where the predictable fate determination of stem cell differentiation through *in vitro* manipulations presents a key strategy. To date, the so-called "conventional osteogenic factors"[9] have empirically been formulated, containing ascorbic acid and beta-glycerophosphate with/without dexamethasone. Furthermore, various growth factors and extrinsic factors have been examined for this purpose[10–13].

The application of bone morphogenetic protein-2 (BMP-2) has been explored for the *in vitro* osteogenic fate-specific differentiation of stem cells. However, BMP-2 has also been shown to differentiate MSC to other lineages, such as adipocytes[14,15]. BMP binds to putative receptors and initiates receptor-regulated Smad phosphorylation. This immediate downstream event was similarly activated during osteogenic[16,17] and adipogenic differentiation[18]. BMPs are multifunctional growth factors in the transforming growth factor super family[19]. It has been shown that the effect of BMP-2 can be modulated through different signaling pathways, such as Ras/MARK system, Hedgehog, cAMP, Notch and Wnt[20,21]. Therefore, multiple co-factors might interact with the BMP-2 signaling pathway, collectively contributing to fate-specific differentiation. However, extrinsic factors that effectively and specifically mediate the differentiation of MSC have not been determined.

The objective of this project was to explore a systematic and computational approach for designing a cocktail of extrinsic factors to stably achieve osteogenic-fate determination of MSC. We applied a feedback system control (FSC) method, using a differential evolution (DE) algorithm, to derive osteogenic cocktails without predisposing

hypotheses. The results showed that FSC rapidly elicited optimized solutions from numerous cocktail candidates. The identified combinations of concentration-specific extrinsic factors induced the osteogenic differentiation of MSC with great efficiency. Surprisingly, one of the effective cocktails contained only 0.39 ng/mL BMP-2, compared with the frequently reported BMP-2 concentration of 100 ng/mL[12,22,23], and yet was capable of activating Smad phosphorylation, resulting in the accelerated *in vitro* mineralization of clonal mouse and primary human MSC.

Results

Feedback system control (FSC) method using a differential evolution (DE) algorithm. FSC rapidly elicits optimized solutions from numerous candidates with great efficiency. In contrast with empirical trial-and-error methods, goal-guided FSC involves four steps: (1) set the physiologically appropriate goals; (2) cautiously select the variable factors; (3) use a high-integrity stochastic algorithm approach to efficiently elicit optimized harmonization from numerous candidates; and (4) formulate a comparative discussion between the results and the physiologic goals. FSC iterations are accomplished using a repeated loop of the interdependent components: the experimental evaluation of the response of the biological system under stimulation and a numerical search algorithm for predicting an improved drug-dosage combination for the next experimental feedback test (Figure 1a).

In the present study, two physiologically appropriate goals, or objective functions, were determined: to facilitate the *in vitro* osteogenic differentiation of MSC and to reduce the dosage of BMP-2. Therefore, we applied a double-objective FSC method to streamline the search for appropriate cocktails.

From previous studies concerning mouse bone marrow MSC cell lines, including C3H10T1/2, MC3T3-E1, C2C12 or ST2 cells[10–13] (Supplementary References of Osteogenic Factors), we selected the following extrinsic factors: BMP-2, synthetic glucocorticoid (dexamethasone; Dex), ascorbic acid (AA or its derivative ascorbic acid-2-phosphate; AA2P), beta-glycerophosphate (beta-GP), heparin (Hep), retinoic acid (RA), and 1,25(OH)$_2$D$_3$ (VD3). Some synthetic derivatives, instead of intrinsic biomolecules, were utilized coincident with conventional osteogenic culture conditions. The reported doses of each extrinsic factor varied significantly (Supplementary Table S1).

Mouse MSC (D1 ORL UVA [D1] or D1 cell, ATCC® Number: CRL-12424™) was selected as a multipotent MSC platform with the capability of expeditious osteogenic fate determination *in vitro*[10,11,24]. Cell culture medium containing 2% or 10% FBS and 1% antibiotics was utilized as the control medium (negative control). Control medium containing a cocktail of traditional osteogenic factors (AA2P: 50 μM, beta-GP: 10 mM and Dex: 100 nM) with BMP-2 (100 ng/ml) was used as a positive control (hereafter denoted as the TB cocktail). To identify the optimal combinatory factors, logarithmic increment doses within the previously published dose range of each extrinsic factor were determined and described as code (Table 1). As a result, these 7 factors and 1 to 10 dose levels or 0 to 12 dose levels generated 10^7 (10.0 million) to 13^7 (62.7 million) theoretical combinations.

A high-integrity stochastic DE algorithm was used in this project. The DE algorithm optimizes problems through iterative improvements in candidate solutions with regard to a given measure of quality. Moreover, this algorithm mimics natural biological evolution. In the present study, the following process was performed: Initially, N (=10 to 14) arbitrary drug cocktails were generated (step 1). For each drug cocktail, a mutated drug cocktail was generated according to a set of mathematical formulae (step 2). Next, the initial drug cocktail and the mutated drug cocktail were crossed to produce a crossover cocktail (step 3), herein referred to as the "test drug cocktail" to emphasize its role in competing against the original drug cocktail. Upon experimental comparison of the original and test drug cocktail, the cocktail that produced better system outcomes (e.g., ALP activity or mineralization index; see below) was selected and used in the next iteration (step 4). After all of the initial drug
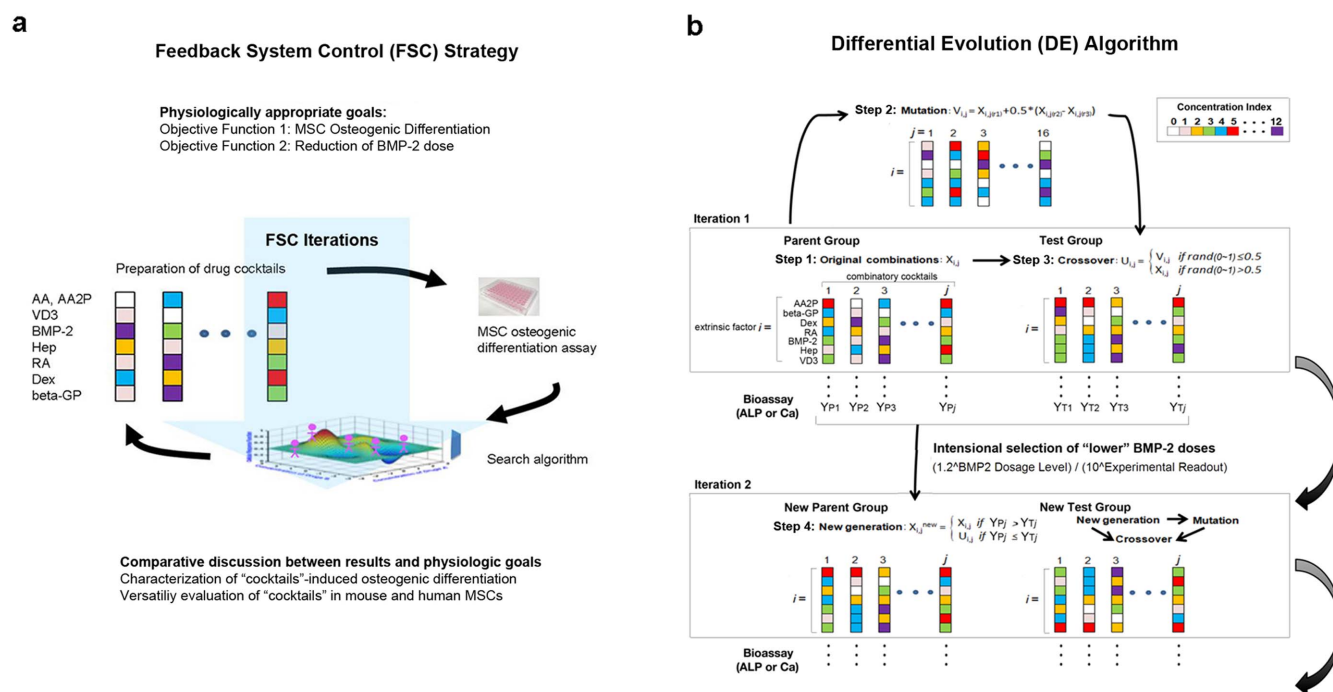

Figure 1 | Schematic diagram of a double objective FSC-DE. (a) Feedback system control (FSC) applied for the identification of combinatory multiple extrinsic factors to determine the differentiation fate of MSC. (b) Differential evolution (DE) used as the search algorithm in this project. Each color represents the concentration of each of the seven extrinsic factors, selected from a scale ranging from 1 to 10 or 0 to 12. The combination of these factors resulted in 10^7 (10 million) or 13^7 (62.7 million) theoretical combinations in the present study.

Table 1 | Code and corresponding concentration for the extrinsic factors used in the double-objective FSC search

Code	12	11	10	9	8	7	6	5	4	3	2	1	0	Unit
Extrinsic Factors														
AA or AA2P	400	200	100	50	25	12.5	6.25	3.13	1.56	0.78	0.39	0.2	0	μM
VD3	80	40	20	10	5	2.5	1.25	0.63	0.31	0.16	0.08	0.04	0	nM
BMP-2	400	200	100	50	25	12.5	6.25	3.13	1.56	0.78	0.39	0.2	0	ng/ml
Hep	400	200	100	50	25	12.5	6.25	3.13	1.56	0.78	0.39	0.2	0	μg/ml
RA	40	20	10	5	2.5	1.25	0.63	0.31	0.16	0.08	0.04	0.02	0	μM
Dex	800	400	200	100	50	25	12.5	6.25	3.13	1.56	0.78	0.39	0	nM
beta-GP	80	40	20	10	5	2.5	1.25	0.63	0.31	0.16	0.08	0.04	0	mM

cocktails underwent mutation (step 2), crossover (step 3) and selection (step 4), the first iteration was complete. Steps 2 to 4 were repeated until the desired drug cocktails were identified (Figure 1b). In addition, between iterations, the "selection" algorithm was added to prefer the candidate cocktail containing lower BMP-2 concentrations (Figure 1b).

FSC with alkaline phosphatase assay. We first selected the expression of alkaline phosphatase (ALP), a widely known osteogenic biomarker, as one of the objective functions of FSC. We constructed the following feedback loop: 1) generate the initial cocktail with a collection of extrinsic factors at arbitrarily selected dosages; 2) apply the cocktail to MSC *in vitro* for 3 days; 3) perform the ALP expression assay; and 4) generate a set of improved new combinations through a DE search algorithm to stimulate the biological system in the next iteration.

After 9 iterations with 20 cocktails tested in each iteration, 8 cocktails among the deferred 180 cocktails (90 actual cocktails) significantly increased ALP expression in D1 cells after 3 days, despite a lower BMP-2 dosage. However, when tested for *in vitro* mineralization, none of these 8 cocktails produced noticeable Ca^{2+} precipitation (Figure 2a), indicating that the identified cocktails did not induce the osteogenic differentiation of MSC. The dose changes along the FSC iteration course indicated that the ALP expression was associated with increased concentrations of RA (Supplementary Fig. S1a). Indeed, 70% of the cocktails generated during FSC, using ALP expression as the objective function, contained the top 2 maximum concentrations of RA (Figure 2b). The adult mouse fibroblastic cell line, L929 (NCTC clone 929 cell, ATCC® Number: CCL-1™), was also shown to induce ALP expression with one of the representative candidate cocktails.

When RA was removed from the cocktail, the ALP expression in D1 and L929 cells was completely abolished, whereas the removal of BMP-2 or VD3 had no effect (Supplementary Fig. S1b). Therefore, the increased ALP expression in MSC and fibroblasts reflected a high dose of RA in the identified cocktails, which obviously failed to direct osteogenic differentiation. Notably, this experiment demonstrated an unintended observation that FSC was in fact capable of rapidly identifying the optimal cocktail for the objective function of ALP expression, in which RA doses approached high doses only after several iterations. However, the identified FSC cocktails did not meet the physiological goal of inducing MSC osteogenic differentiation.

FSC with *in vitro* mineralization assay. We selected *in vitro* mineralization as the objective function in the second experiment, based on measuring the level of Ca^{2+} precipitation in the wells on day 7. In this search, we examined 24 drug cocktails per iteration. Through 9 iterations, FSC generated a deferred total of 216 cocktails (100
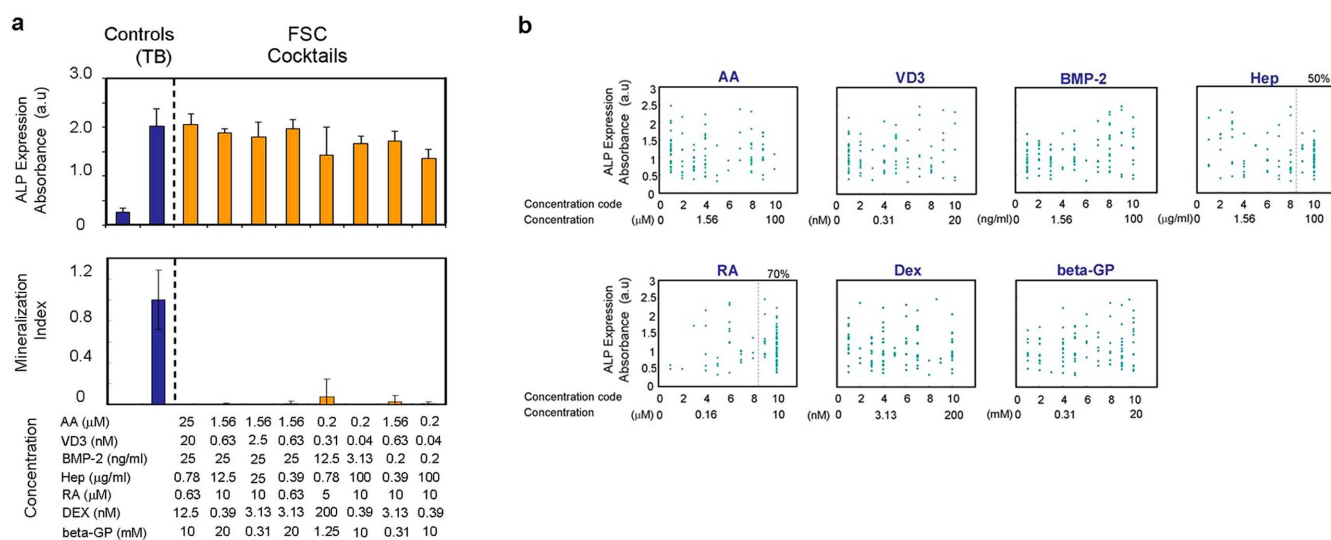

Figure 2 | FSC-DE with ALP assay. (a) Effect of prospective drug cocktails identified with FSC-DE with ALP assay from 10 million potential candidates for the osteoblastogenesis of D1 cells. The prospective cocktails did not induce *in vitro* mineralization, despite high ALP activity. (b) Correlation between doses of extrinsic factors in each drug cocktail elicited and used in FSC-DE with ALP assay against ALP expression in D1 cells. Dots: each drug cocktail. All data represent the actual measurement values in the FSC-DE process. The highest concentration codes 9 and 10 of RA were involved in 70% of all FSC-generated cocktails. D1 cells were seeded at 3125/cm², and the ALP activity was measured on day 3. Note that the prospective drug cocktails in Figure 2a were narrowed using setting gates with the following criteria: BMP-2 code less than 9 and ALP activity above 1.5. (a, b) Bar graphs and dots show the mean with/without s.d. of three independent determinations. Each concentration of extrinsic factors represents the one in drug cocktails and does not include the one in FBS.

actual cocktails). Fourteen cocktails demonstrated *in vitro* Ca^{2+} precipitation within 7 days, achieving greater than 50% of the mineralization index (Ca^{2+} precipitation in D1 cell culture containing a given cocktail per that with TB) (Figure 3a & Supplementary Fig. S2). Four of these drug cocktails contained a BMP-2 dosage of 12.5% or less relative to that in TB, but these cocktails were capable of inducing *in vitro* mineralization, even under diluted cell seeding conditions (Figure 3b).

The mineralization index was positively correlated with increasing concentrations of AA2P and beta-GP, and inversely correlated with RA, Hep and VD3. However, BMP-2 and Dex, potent osteogenic factors, did not show noticeable correlations (Figure 3c). When small variations of the VD3 doses were introduced, the osteogenic capability of one of FSC cocktail, m8T11, was impaired (Figure 3d), suggesting that the identified doses of each factor might play unique roles in the osteogenic differentiation of MSC.

Characterization of the identified cocktails. The representative cocktails m8T11 and m4T5 (Table 2) were selected for further

investigation. *Taqman*-based real-time reverse transcription polymerase chain reaction (RT-PCR) showed that both TB and m8T11 induced the early expression of *Runx2* and *Osx* (Day 1) and the delayed expression of osteocalcin (*Ocn*) (Day 7) (Figure 4a). The m4T5 cocktail also induced *Runx2* and *Osx*, albeit with a different expression pattern. The upregulated ALP expression (Figure 4b) and the lack of effect on L929 fibroblasts (Supplementary Fig. S3) further suggested that these cocktails achieved the osteogenic fate determination of MSC.

BMPs are extrinsic factors that bind to their putative receptors and initiate the phosphorylation of the receptor-regulated Smads[16], which is critical for stem cell osteogenic differentiation[25,26]. The BMP-2 dose (code 2, 0.39 ng/ml) in the m8T11 cocktail was only 1/256 of that in TB (100 ng/ml). Therefore, we examined whether media containing m4T5 and m8T11 cocktails initiated the BMP-Smad signaling pathway using antagonist molecules: Noggin, which interferes with the receptor association of TGF-beta family ligands, including BMPs; and Dorsomorphin (Dorso), which blocks BMP-mediated Smad activation[27].
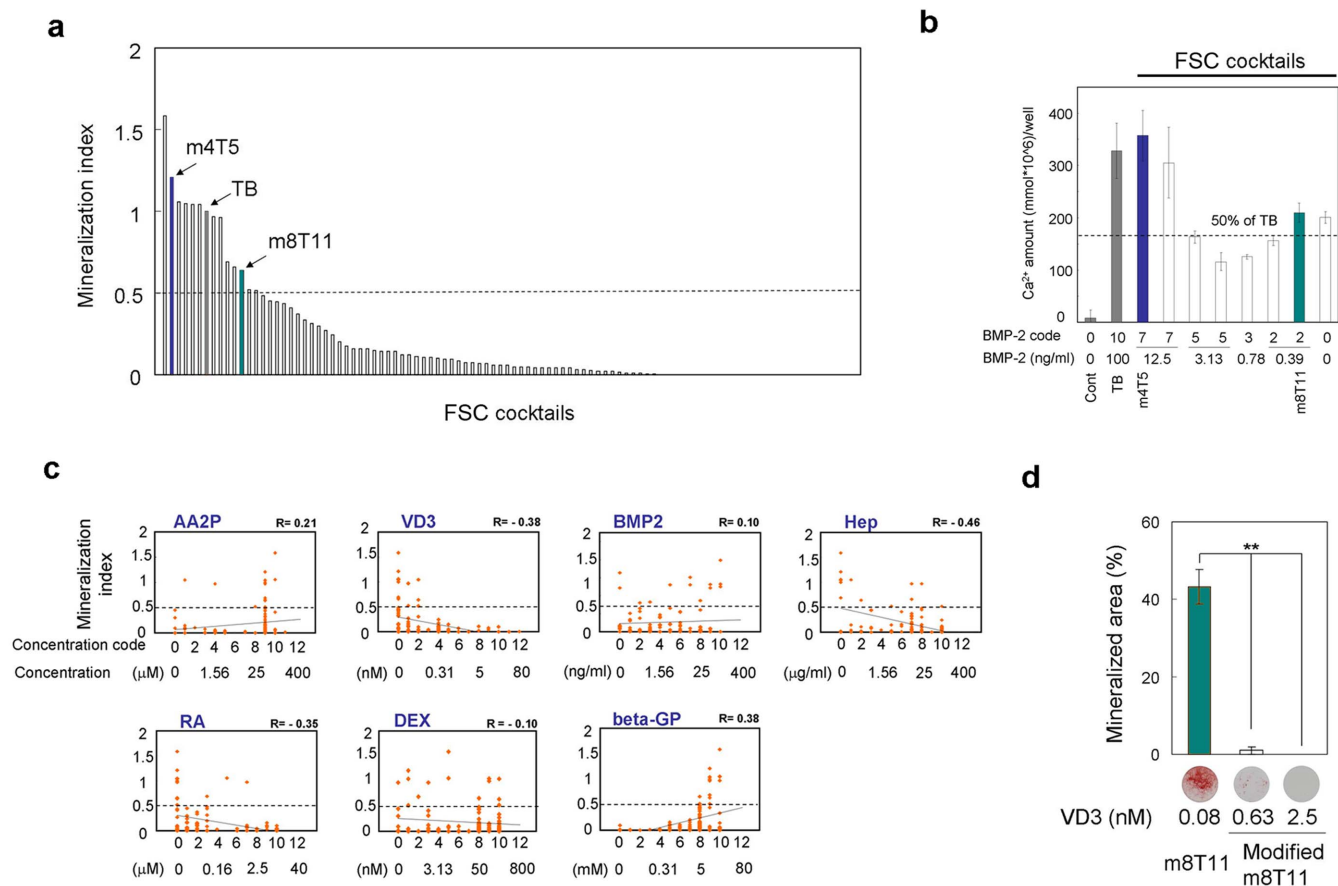

Figure 3 | Identification of prospective drug cocktails using FSC-DE with mineralization assay. (a) Arrangement of the drug cocktails in the order of each mineralization index. The break line represents the threshold mineralization index of 0.5. D1 cells were seeded at 45,000/cm²; once the cells were confluent, the media were changed to basal media and subsequently changed to media containing each drug cocktail. The Ca^{2+} content was measured on day 7. (b) Mineralization assay using the prospective cocktails within the following gate and the diluted cell-seeding condition. D1 cells were seeded at 3125/cm²; the media were changed to media containing each drug cocktail on day 1, and the Ca^{2+} content in the well was measured on day 15. Gate: BMP-2 code less than 8 and mineralization index above 0.5. (c) Correlation between the doses of the extrinsic factors in each drug cocktail against the mineralization index. Dots: each drug cocktail elicited and used in FSC-DE with mineralization assay. All data represent actual measurement values in the FSC-DE process. The dots show the mean of three independent determinations. R: Correlation coefficient. Line: Linear correlation. (d) The effect of VD3 modifications in m8T11. Bar graph: quantitative mineralization assay with original m8T11 (VD3 code 2) and modified m8T11 (VD3 code 5 and 7). D1 cells were seeded at 45,000/cm²; once the cells were confluent, the media were changed to basal media and subsequently changed to media containing each drug cocktail. The mineralized area was measured on day 7. **: P < 0.01 (ANOVA with a Dunnett's test). Representative Alizarin red-stained images. (a, b, d) The bar graphs shows mean with/without s.d. of three independent determinations. Each concentration of extrinsic factors represents the one in drug cocktails and does not include the one in FBS.

Qualitatively, Noggin treatment selectively decreased the small Alizarin red-positive areas, revealing trabecular patterns (Figure 4c). Both Noggin and Dorso treatments significantly decreased the *in vitro* mineralization of the media containing TB and m4T5 cocktails (Figure 4c, d). However, the MSC behaviors with m8T11 medium were different. The significant attenuation of m8T11-induced *in vitro* mineralization was only achieved with Dorso, but not with Noggin (Figure 4c, d). BMP-2 binds to the high affinity receptor, BMP receptor type I (BMPR1), and subsequently recruits BMPR2, resulting in the formation of a receptor heterodimer or oligomer[16]. RT-PCR revealed the early increase and sustained expression of endogenous *Bmp-2* and its receptors, *Bmpr1A* and *Bmpr2*, with m8T11 medium. TB and m4T5 media showed a late increase in the expression of *Bmp-2* and its receptors (Figure 4e).

Osteogenic-fate differentiation of primary human MSC with m8T11. We investigated whether m4T5 and m8T11 cocktails were also effective for the osteogenic differentiation of primary human MSC (hMSC) (Figure 5). Consistent with the results using mouse MSC D1 cells, we observed that the m8T11 cocktail effectively induced *in vitro* mineralization in primary hMSC, while the m4T5 cocktail did not (Figure 5a, 5b). The representative conventional osteogenic medium containing 250 μM AA2P, 10 mM beta-GP, and 10 or 100 nM Dex (Conv-OM) was less effective than the m8T11 cocktail in inducing the *in vitro* mineralization of hMSC.

Discussion

This study demonstrated the use of a double-objective FSC technique for the rapid identification of supplement combinations exhibiting the versatile osteogenic differentiation of MSC. The FSC strategy has previously been used for eradicating viral infections[28], controlling herpes virus reactivation[29], and maintaining human ES cells[30]. This method facilitates the identification of optimal drug combinations without any predisposing hypotheses. A recent study reported the unintended FSC-mediated selection of drug cocktails predominantly containing Ribavirin at high doses using HSV-1-infected NIH3T3 fibroblasts as a biological assay model. We similarly experienced that the FSC iterations using ALP expression as a biological assay model converged high dose RA as a single effective factor. However, in the present study, these FSC cocktails did not induce the intended physiological outcome of MSC osteogenic differentiation. These results underscore the robust effectiveness of FSC but indicate the limitations of this strategy due to the sensitivity and disproportionate reliance on the biological assay design.

Using *in vitro* mineralization as an alternative objective function, we successfully identified two extrinsic factor combinations, m4T5 and m8T11. The FSC formula developed for the present study included the command with the "code 0" or exclusion of the putative factor. This built-in mechanism facilitated the elimination of components that did not contribute to the biological outcome. Indeed, the identified FSC cocktails, m4T5 and m8T11, did not contain RA (Table 2), which induced artificial ALP expression. Notably, both m4T5 and m8T11 induced ALP expression without RA (Figure 4b), indicating the osteogenic differentiation of MSC.

Mutant mice lacking *Runx2*[31,32] or osterix (*Osx*)[33] have been shown to exhibit the complete arrest of bone formation, suggesting that these intrinsic factors determine osteogenic fate. Furthermore, the gene transcription of the osteoblast-specific molecule, osteocalcin (*Ocn*), is regulated through *Runx2* and *Osx*[34]. The early upregulation of *Runx2* and *Osx* has been used as an indicator of osteogenic differentiation. The m8T11 cocktail demonstrated a sequential gene expression pattern associated with osteogenic differentiation, whereas m4T5 delayed the expected gene expression (Figure 4a).

Notably, m4T5 and m8T11 contained 12.5 and 0.39 ng/mL BMP-2, respectively, compared with the 100 ng/mL BMP-2 concentration commonly reported for *in vitro* studies[12,22,23] (Table 2). Considering serum BMP-2 levels of 1.0 ng/mL or 0.09 ng/mL in mice and humans, respectively, the FSC cocktails utilized in the present study represent a more physiological environment than previously reported osteogenic conditions. BMP-2 and BMP-7 have been accepted for marketing to assist ectopic bone formation and bone repair[35]. Studies have shown that the supra-physiological dose of BMP-2 (1.5 mg/mL) required to achieve a therapeutic effect has been associated, in part, with high healthcare costs and possible serious side effects that might limit wider clinical use[36]. The current FSC iteration demonstrated that *in vitro* mineralization occurred, irrespective of BMP-2 concentration (Figure 3c). Further characterization of m4T5 and m8T11 demonstrated the activation of BMP-2 receptor-regulated Smad cascade (Figure 4c and 4d), suggesting that BMP-2 elicited the expected effects, despite low concentrations.

Studies evaluating the effectiveness of BMPs and Dex have shown that rodent and human MSC responded differently to osteogenic

Table 2	Concentration of Osteogenic Factors in Physiologic Serum/Plasma and Differentiation Media							
	Physiological concentration in mouse serum (plasma)	Physiological concentration in human serum (plasma)	Conventional concentration reported in the literature*	TB[i] medium (without FBS)	m4T5[i] medium (without FBS)	m8T11[i] medium (without FBS)	2% FBS	10% FBS
AA or AA2P (μM)	44.6[a,(R1)]	51.7[a,(R2)]	50[b], 250[b], 238.38[a]	50[b]	50[b]	50[b]	0.35[a,c,f,(R3)]	1.75[a,c,g,(R3)]
VD3 (nM)	0.102[(R4)]	0.1[(R5)]	10	0	0	0.08	0.0008[c,f,(R6)]	0.0039[c,g,(R6)]
BMP-2 (ng/mL)	1[(R7)]	0.09[(R8)]	100	100	12.5	0.39	0.012[f,(R9)]	0.06[g,(R9)]
Hep (μg/mL)	-	1 ~ 2.4[c,(R10)]	10	0	0	0.39	-	-
RA (nM)	~2[(R11)], 3.6[(R12)]	4.6[(R12)], ~14[(R13)]	1000	0	0	0	0.72 ~ 1.26[f,(R14)]	3.6 ~ 6.2[(R14)]
GC or Dex (nM)	87 ~ 320[c,d,(R15,16)]	200[e,(R17)]	10	100	0.39	200	1.7[c,d,f,(R18)], 4[c,e,f,(R18)]	8.5[c,d,g,(R18)], 20[c,e,g,(R18)]
Serum phosphate or beta-GP (mM)	2.7[h,(R19)]	0.8 ~ 1.4[h,(R20)]	10	10	10	10	0.046[h,f,(R21)]	0.23[h,g,(R21)]

[a]As AA.
[b]As AA2P; The effective concentration of AA2P for human osteoblast-like cell is similar to that of AA (R22).
[c]In plasma.
[d]As corticosterone.
[e]As cortisol (hydrocortisone).
[f]One-fifth or fiftieth of the original number in the reference.
[g]One-tenth of the original number in the reference.
[h]As serum phosphate or phosphorus.
[i]Basal media with each drug cocktail; At MSC osteogenic differentiation assay, these media contained 2 and 10% FBS.
*References in the main text and Supplementary references of osteogenic factors.
(R number): Reference number in the Supplementary reference list for Table 2.
GC: Glucocorticoid. The efficacies of the two hormones for osteoblastogenesis are similar to that of Dex (R23, R24).
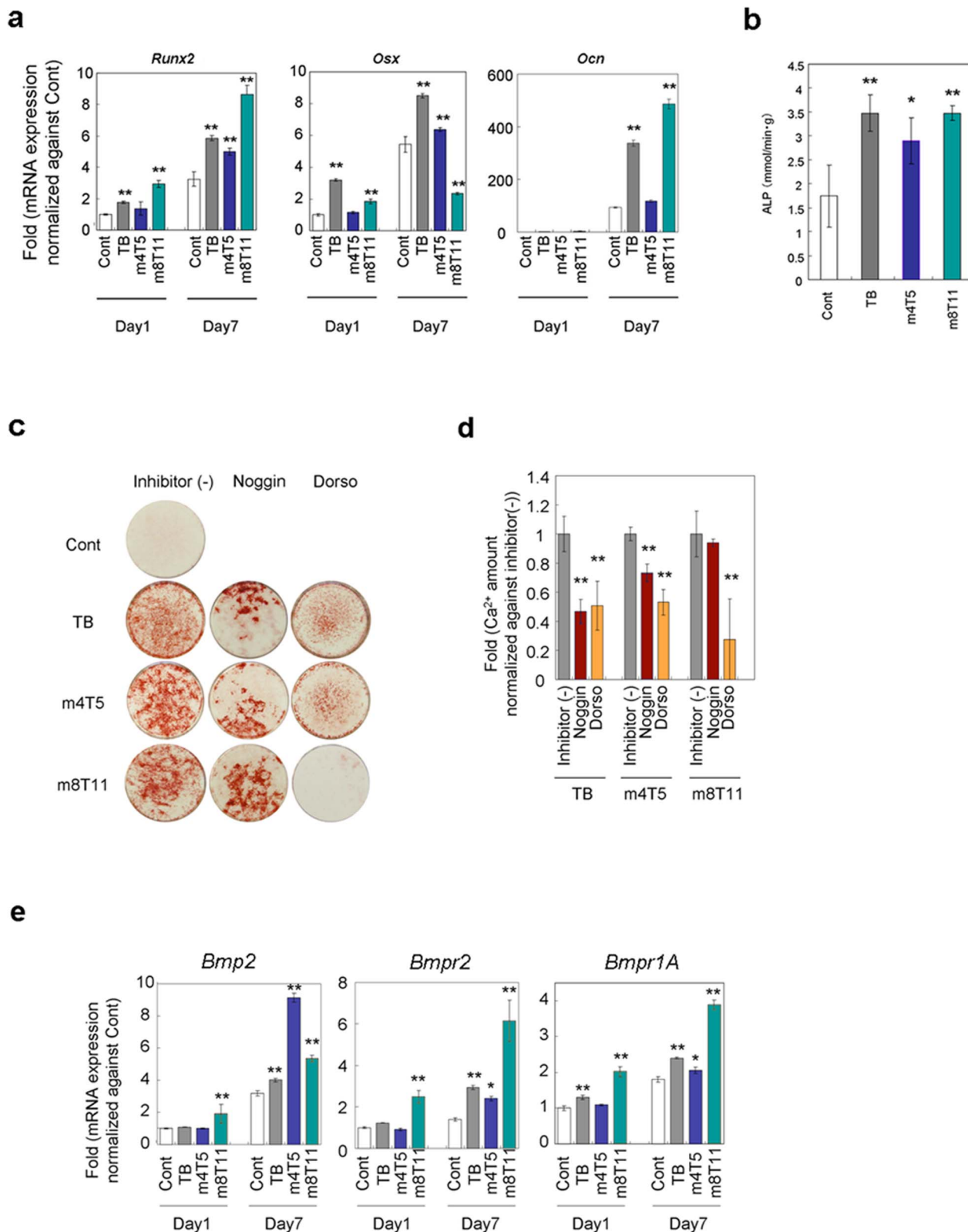
Figure 4 | Osteoblastogenesis induced by m4T5 and m8T11 cocktail and BMP-SMAD signaling pathway. (a) Taqman-based real-time reverse transcription polymerase chain reaction for Runx2, Osx and Ocn. **: $p < 0.01$ compared with the control (ANOVA with a Dunnett's test). (b) ALP expression in the well measured on day 7. *: $p < 0.05$ and **: $p < 0.01$ compared with the control (ANOVA with a Dunnett's test). (c) Alizarin red staining of D1 cells treated with drug cocktails with/without the following inhibitors: 500 ng/ml of Noggin and 5 μM Dorsomorphin (Dorso). The mineralized matrix was stained with Alizarin red S on Day 7. (d) Quantitative mineralization assay with BMP-SMAD pathway inhibitors. **: $p < 0.01$ compared with each inhibitor ($-$) (ANOVA with a Dunnett's test). (e) Effect of drug cocktails on mRNA expression of Bmp2, Bmpr2 and Bmpr1A. *: $p < 0.05$ and **: $p < 0.01$ compared with the control (ANOVA with a Dunnett's test). In all experiments, D1 cells were seeded at 45,000/cm²; once the cells became confluent, the media were changed to basal media and subsequently changed to media containing each drug cocktail. The bar graphs show the mean with s.d. of three independent determinations.
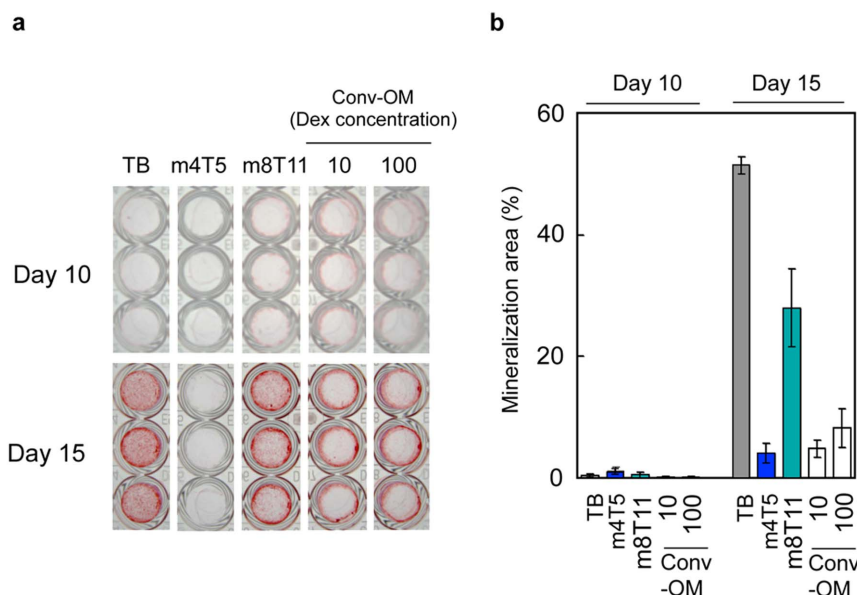
a

b

Figure 5 | Osteogenic effect of m4T5 and m8T11 for primary human MSC. (a) Alizarin red-stained human MSC cultures treated with TB (containing 100 ng/mL BMP-2), FSC cocktails m4T5 or m8T11, or conventional osteogenic media (Conv-OM: containing 10 nM or 100 nM Dex). On culture day 15, the m8T11 cocktail induced alizarin red-positive mineralized nodules, while m4T5 did not. (b) The alizarin red-positive area measurement (excluding the peripheral ring) suggested that the effect of m8T11 on the osteogenic differentiation of human MSC was approximately 50% of that with TB and greater than 300% of that with Conv-OM.

differentiation environments *in vitro*[37,38]. In the present study, we also observed the differential effectiveness of the FSC cocktails on the osteogenic differentiation of human MSC. While both m4T5 and m8T11 contained BMP-2, only m8T11 induced the *in vitro* mineralization of human MSC (Figure 5). The m8T11 cocktail contained the extracellular molecules, Hep and VD3 (Table 2). Hep might protect BMP-2 from Noggin and support BMP-2-derived osteogenic differentiation[13], which might partially explain the ineffectiveness of Noggin in m8T11. VD3 alone[39] or the combination of VD3 and BMP-2[40] has been shown to increase *Ocn* expression, whereas a chromatin immunoprecipitation microarray analysis of MSC revealed that VDR-derived chromatin remodeling might suppress gene transcription[41,42]. It is highly conceivable that the effect of VD3 on the osteogenic differentiation might be dose-sensitive.

The dose of extrinsic factors in the medium containing m8T11 cocktail with FBS were near the range of physiological concentrations observed in mouse and human serum (Table 2). Considering that the identified cocktails contain derivatives instead of biomolecules and lack various other extrinsic factors, it might be possible to reconstruct this intact biological osteogenic phenomenon *in vivo*. However, the newly identified cocktails might provide a novel opportunity to elucidate the molecular mechanisms of MSC osteogenic differentiation in a physiologically relevant context.

The recent development of the potential use of induced pluripotent stem cells (iPSC) should broaden the application of the stem cell-based disease modeling[43–45]. For example, BMP has been shown to induce ectopic ossification leading to atherosclerosis[46]. The significantly reduced BMP-2 doses in the identified cocktails and the near-physiological environment might contribute to the modeling of vascular cell calcification without potentially confounding the BMP-2-derived proinflammatory reaction[47].

In conclusion, in the present study, we demonstrated the use of a FSC for the rapid identification of cell culture supplement combinations exhibiting BMP-induced osteogenic differentiation through extrinsic factors. The outcome of this study might provide a basis for stem cell-based disease modeling and putative drug development using high throughput screening.

Methods

Cell maintenance. The mouse MSC line (D1 ORL UVA [D1], D1 cell, CRL-12424), derived from bone marrow, and the mouse fibroblastic cell line (NCTC clone 929 cell, L-929 cell, CCL-1), derived from subcutaneous connective tissue, were purchased from the American Type Culture Collection (ATCC, Manassas, VA, USA). D1 cells exhibit specific MSC surface markers and are capable of developing osteogenic, chondrogenic and adipogenic differentiation[24]. The cells lines were maintained at subconfluence in Dulbecco's Modified Essential Medium (DMEM) supplemented with 10% fetal bovine serum (FBS) and 1% antibiotics in a 5% CO$_2$ incubator at 37°C. The cells were used for the assays at passages 3 to 6. Primary hMSC, obtained from normal human bone marrow, were commercially purchased from Lonza Walkersville, Inc. (Walkersville, MD, USA, Product No PT-2501). The cells were maintained at subconfluence in MSCGMTM (Lonza Walkersville, Inc., Walkersville, MD, USA) growth medium in a 5% CO$_2$ incubator at 37°C. According to the manufacturer's instructions, the cells at passage 3 (not exceeding passage 5) were used for assays.

Drug cocktail preparation. Ascorbic acid (AA) or ascorbic acid 2 phosphate (AA2P), Beta-glycerophosphate (beta-GP), Dexamethasone (Dex), Retinoic acid (RA) and Heparin (Hep) were purchased from Sigma-Aldrich (St. Louis, MO, USA). 1,25(OH)$_2$D$_3$ (VD3) was obtained from EMD Chemicals Inc. (Gibbstown, NJ, USA). Recombinant human BMP-2 was obtained from R&D Systems (Minneapolis, MN, USA) and PeproTech (Rocky Hill, NJ, USA). BMP-2 and the other six ingredients at various concentrations were mixed in DMEM containing 1% antibiotics and FBS (2% for D1 cell and L929 cell, 10% for hMSC), and these mixtures were used as prototypes for the media containing drug cocktails (Table 1). The code of ingredients represents the concentration of each reagent in the drug cocktails (Table 1).

Quantitative ALP activity assay. ALP activity was determined with a biochemical colorimetric assay. The cells were briefly washed with PBS and lysed with RIPA buffer. The enzymatic ALP activity in the lysate was assayed by measuring the *p*-nitrophenol formed from the enzymatic hydrolysis of *p*-nitrophenylphosphate, as a substrate, at 405 nm. In some cases, ALP data were normalized against the total protein quantity measured using the BCA protein assay reagent kit (Pierce, Rockford, IL, USA).

Quantitative real-time PCR. Total RNA from D1 cell cultures was isolated using the RNeasy Plus Mini Kit (Qiagen Inc., Valencia, CA, USA). The steady-state mRNA levels were determined through TaqMan-based real-time PCR using the Taqman Gene Expression assay with the following probe/primer combinations: *Runx2*, Mm03003491_m1; *Osx*, Mm04209856_m1; bone gamma-carboxyglutamic acid-containing protein (osteocalcin:*Ocn*), Mm03413826_mH; *Bmp2*, Mm01340178_m1; *Bmpr1A*, Mm00477650_m1; and *Bmpr2*, Mm00432134_m1, *Gapdh*, Mm99999915_g1. The mRNA expression levels were normalized using the comparative CT method.

Quantitative Ca²⁺ assay and mineralization index. Ca^{2+} accumulation in each well was evaluated as the degree of mineralization. The cells were washed twice with PBS and decalcified with 0.5 N HCl, and the cell culture plates were rotated for 4 h at 4°C. The Ca^{2+} content in the supernatant was estimated against the standard provided in the LiquiColor kit (Stanbio Laboratories, Boerne, Texas, USA). The reaction between Ca^{2+} and ortho-cresolpthalein complex produces a purple complex measured at 550 nm, and the color intensity is directly proportional to the concentration of calcium in the sample. Basal DMEM with FBS and antibiotics were utilized as the control medium (negative control). TB: Control medium containing traditional osteogenic factors (50 μM AA2P, 10 mM beta-GP and 100 nM Dex) with a high dose BMP-2 (100 ng/ml) was adopted as a benchmark. The mineralization indexes were calculated using the quantity of Ca^{2+} accumulation induced by the samples per those of TB.

Alizarin red staining. To evaluate the mineralized bone nodules, the cultured cells were stained with Alizarin red S (Sigma-Aldrich, St. Louis, MO, USA). The cell layers were fixed in absolute ethanol for 10 min, washed with ddH₂O, and stained with 1% Alizarin red S. After 30 min, the cell layers were repeatedly washed with ddH₂O. The images were captured using a Canon A495 camera. The prescribed central parts of the wells were scanned and analyzed using Image J software to quantify the average percentage of mineralization area against the surface area (i.e., Edges of the wells were excluded from this calculation).

BMP/SMAD signaling pathway inhibitors. Murine Noggin was purchased from Pepro Tech (Rocky Hill, NJ, USA). Dorsomorphin (Dorso) was obtained from Calbiochem (San Diego, CA, USA). The cells were treated with drug cocktails containing 500 ng/ml of noggin or 5 μM Dorso to determine whether the BMP-SMAD signaling pathway is involved in the osteoblastogenesis induced through the drug cocktails.

Feedback system control (FSC) with differential evolution (DE) algorithm. FSC was performed as follows: D1 cells were stimulated with different drug cocktails. The level of ALP activity or mineral index was measured and used as an objective function to observe the osteogenic effect of each drug cocktail. The results were fed into the DE stochastic search algorithm, which elicited the composition of the new drug cocktail candidates for the next bioassay. MATLAB software (MathWorks Inc., Natick, MA, USA) was used to code the DE algorithm, in which each drug cocktail was represented as a vector. We used a coded dosage instead of the absolute concentration. The new drug cocktails were manually prepared and utilized to perform the next bioassay, and this process was repeated until the optimal drug cocktails were obtained.

Statistical analysis. Statistical significance was assessed using one-way analysis of variance, followed by Dunnett's multiple comparisons test. The Microsoft Excel software statistic package was used for the calculation.

1. Colman, A. & Dreesen, O. Pluripotent stem cells and disease modeling. *Cell stem cell* **5**, 244–247 (2009).
2. Augello, A., Kurth, T. B. & De Bari, C. Mesenchymal stem cells: a perspective from in vitro cultures to in vivo migration and niches. *Eur Cell Mater* **20**, 121–133 (2010).
3. Rodriguez, J. P., Montecinos, L., Rios, S., Reyes, P. & Martinez, J. Mesenchymal stem cells from osteoporotic patients produce a type I collagen-deficient extracellular matrix favoring adipogenic differentiation. *J Cell Biochem* **79**, 557–565 (2000).
4. Liu, Y. *et al.* Intracellular VEGF regulates the balance between osteoblast and adipocyte differentiation. *J Clin Invest* **122**, 3101–3113 (2012).
5. Szpalski, C., Barbaro, M., Sagebin, F. & Warren, S. M. Bone tissue engineering: current strategies and techniques--part II: Cell types. *Tissue Eng Part B Rev* **18**, 258–269 (2012).
6. Mohal, J. S., Tailor, H. D. & Khan, W. S. Sources of adult mesenchymal stem cells and their applicability for musculoskeletal applications. *Curr Stem Cell Res Ther* **7**, 103–109 (2012).
7. Brey, D. M. *et al.* High-throughput screening of a small molecule library for promoters and inhibitors of mesenchymal stem cell osteogenic differentiation. *Biotechnol Bioeng* **108**, 163–174 (2011).
8. Alves, H., Dechering, K., Van Blitterswijk, C. & De Boer, J. High-throughput assay for the identification of compounds regulating osteogenic differentiation of human mesenchymal stromal cells. *PLoS One* **6**, e26678 (2011).
9. Hoemann, C. D., El-Gabalawy, H. & McKee, M. D. In vitro osteogenesis assays: influence of the primary cell source on alkaline phosphatase activity and mineralization. *Pathol Biol* **57**, 318–323 (2009).
10. Hsiong, S. X., Boontheekul, T., Huebsch, N. & Mooney, D. J. Cyclic arginine-glycine-aspartate peptides enhance three-dimensional stem cell osteogenic differentiation. *Tissue Eng Part A* **15**, 263–272 (2009).
11. Kim, H. K. *et al.* Red light of 647 nm enhances osteogenic differentiation in mesenchymal stem cells. *Lasers Med Sci* **24**, 214–222 (2009).
12. Siddappa, R. *et al.* cAMP/PKA signaling inhibits osteogenic differentiation and bone formation in rodent models. *Tissue Eng Part A* **15**, 2135–2143 (2009).
13. Zhao, B. *et al.* Heparin potentiates the in vivo ectopic bone formation induced by bone morphogenetic protein-2. *J Biol Chem* **281**, 23246–23253 (2006).
14. Zehentner, B. K., Leser, U. & Burtscher, H. BMP-2 and sonic hedgehog have contrary effects on adipocyte-like differentiation of C3H10T1/2 cells. *DNA Cell Biol* **19**, 275–281 (2000).
15. Sottile, V. & Seuwen, K. Bone morphogenetic protein-2 stimulates adipogenic differentiation of mesenchymal precursor cells in synergy with BRL 49653 (rosiglitazone). *FEBS Lett* **475**, 201–204 (2000).
16. Liu, F. *et al.* A human Mad protein acting as a BMP-regulated transcriptional activator. *Nature* **381**, 620–623 (1996).
17. Massague, J., Seoane, J. & Wotton, D. Smad transcription factors. *Genes Dev* **19**, 2783–2810 (2005).
18. Hata, K. *et al.* Differential roles of Smad1 and p38 kinase in regulation of peroxisome proliferator-activating receptor gamma during bone morphogenetic protein 2-induced adipogenesis. *Mol Biol Cell* **14**, 545–555 (2003).
19. Wozney, J. M. *et al.* Novel regulators of bone formation: molecular clones and activities. *Science* **242**, 1528–1534 (1988).
20. Chen, G., Deng, C. & Li, Y. P. TGF-beta and BMP signaling in osteoblast differentiation and bone formation. *Int J Biol Sci* **8**, 272–288 (2012).
21. Lin, G. L. & Hankenson, K. D. Integration of BMP, Wnt, and notch signaling pathways in osteoblast differentiation. *J Cell Biochem* **112**, 3491–3501 (2011).
22. Osyczka, A. M. & Leboy, P. S. Bone morphogenetic protein regulation of early osteoblast genes in human marrow stromal cells is mediated by extracellular signal-regulated kinase and phosphatidylinositol 3-kinase signaling. *Endocrinology* **146**, 3428–3437 (2005).
23. Wang, Y. K. *et al.* Bone morphogenetic protein-2-induced signaling and osteogenesis is regulated by cell shape, RhoA/ROCK, and cytoskeletal tension. *Stem Cells Dev* **21**, 1176–1186 (2012).
24. Mussano, F. *et al.* Differential effect of ionizing radiation exposure on multipotent and differentiation-restricted bone marrow mesenchymal stem cells. *J Cell Biochem* **111**, 322–332 (2010).
25. Bais, M. V. *et al.* BMP2 is essential for post natal osteogenesis but not for recruitment of osteogenic stem cells. *Bone* **45**, 254–266 (2009).
26. Javed, A. *et al.* Structural coupling of Smad and Runx2 for execution of the BMP2 osteogenic signal. *J Biol Chem* **283**, 8412–8422 (2008).
27. Anderson, G. J. & Darshan, D. Small-molecule dissection of BMP signaling. *Nat Chem Biol* **4**, 15–16 (2008).
28. Ding, X. *et al.* Cascade search for HSV-1 combinatorial drugs with high antiviral efficacy and low toxicity. *Int J Nanomedicine* **7**, 2281–2292 (2012).
29. Sun, C. P. *et al.* Integrative systems control approach for reactivating Kaposi's sarcoma-associated herpesvirus (KSHV) with combinatory drugs. *Integr Biol (Camb)* **1**, 123–130 (2009).
30. Tsutsui, H. *et al.* An optimized small molecule inhibitor cocktail supports long-term maintenance of human embryonic stem cells. *Nat Commun* **2**, 167 (2011).
31. Komori, T. *et al.* Targeted disruption of Cbfa1 results in a complete lack of bone formation owing to maturational arrest of osteoblasts. *Cell* **89**, 755–764 (1997).
32. Otto, F. *et al.* Cbfa1, a candidate gene for cleidocranial dysplasia syndrome, is essential for osteoblast differentiation and bone development. *Cell* **89**, 765–771 (1997).
33. Nakashima, K. *et al.* The novel zinc finger-containing transcription factor osterix is required for osteoblast differentiation and bone formation. *Cell* **108**, 17–29 (2002).
34. Franceschi, R. T., Ge, C., Xiao, G., Roca, H. & Jiang, D. Transcriptional regulation of osteoblasts. *Ann N Y Acad Sci* **1116**, 196–207 (2007).
35. De Biase, P. & Capanna, R. Clinical applications of BMPs. *Injury* **36 Suppl 3**, S43–46 (2005).
36. Shimer, A. L., Oner, F. C. & Vaccaro, A. R. Spinal reconstruction and bone morphogenetic proteins: open questions. *Injury* **40 Suppl 3**, S32–38 (2009).
37. Diefenderfer, D. L., Osyczka, A. M., Reilly, G. C. & Leboy, P. S. BMP responsiveness in human mesenchymal stem cells. *Connect Tissue Res* **44 Suppl 1**, 305–311 (2003).
38. Osyczka, A. M., Diefenderfer, D. L., Bhargave, G. & Leboy, P. S. Different effects of BMP-2 on marrow stromal cells from human and rat bone. *Cells Tissues Organs* **176**, 109–119 (2004).
39. Sierra, J. *et al.* Regulation of the bone-specific osteocalcin gene by p300 requires Runx2/Cbfa1 and the vitamin D3 receptor but not p300 intrinsic histone acetyltransferase activity. *Mol Cell Biol* **23**, 3339–3351 (2003).
40. Jorgensen, N. R., Henriksen, Z., Sorensen, O. H. & Civitelli, R. Dexamethasone, BMP-2, and 1,25-dihydroxyvitamin D enhance a more differentiated osteoblast phenotype: validation of an in vitro model for human bone marrow-derived primary osteoblasts. *Steroids* **69**, 219–226 (2004).
41. Yuan, W. *et al.* 1,25-dihydroxyvitamin D3 suppresses renin gene transcription by blocking the activity of the cyclic AMP response element in the renin gene promoter. *J Biol Chem* **282**, 29821–29830 (2007).
42. Kato, S., Fujiki, R., Kim, M. S. & Kitagawa, H. Ligand-induced transrepressive function of VDR requires a chromatin remodeling complex, WINAC. *J Steroid Biochem Mol Biol* **103**, 372–380 (2007).
43. Egawa, N. *et al.* Drug screening for ALS using patient-specific induced pluripotent stem cells. *Sci Transl Med* **4**, 145ra104 (2012).
44. Tanaka, T. *et al.* Induced pluripotent stem cells from CINCA syndrome patients as a model for dissecting somatic mosaicism and drug discovery. *Blood* **120**, 1299–1308 (2012).

45. Quarto, N. *et al*. Skeletogenic phenotype of human Marfan embryonic stem cells faithfully phenocopied by patient-specific induced-pluripotent stem cells. *Proc Natl Acad Sci U S A* **109**, 215–220 (2012).

46. Cai, J., Pardali, E., Sanchez-Duffhues, G. & ten Dijke, P. BMP signaling in vascular diseases. *FEBS Lett* **586**, 1993–2002 (2012).

47. Csiszar, A., Labinskyy, N., Jo, H., Ballabh, P. & Ungvari, Z. Differential proinflammatory and prooxidant effects of bone morphogenetic protein-4 in coronary and pulmonary arterial endothelial cells. *Am J Physiol Heart Circ Physiol* **295**, H569–577 (2008).

Acknowledgments

Author contributions

I.N., C.H., Y.H. and X.D. designed the experiments. Y.H., X.D., F.M. and A.W. performed and analyzed the experiments. I.N. and Y.H. drafted the manuscript. All authors discussed the results and commented on the manuscript. I.N. supervised the project.

Additional information

Supplementary information accompanies this paper at http://www.nature.com/scientificreports

Competing financial interests: The authors declare no competing financial interests.

How to cite this article: Honda, Y. *et al*. Guiding the osteogenic fate of mouse and human mesenchymal stem cells through feedback system control. *Sci. Rep.* **3**, 3420; DOI:10.1038/srep03420 (2013).